Supporting Information for:

Microbial dynamics of biosand filters and contributions of the microbial food web to effective treatment of wastewater-impacted water sources

Tara M. Webster[a], Noah Fierer[ab#]

[a]Center for Interdisciplinary Research in Environmental Sciences, University of Colorado, Boulder, CO, 80309, United States

[b]Department of Ecology and Evolutionary Biology, University of Colorado, Boulder, CO 80309, United States

11 pages, 8 Figures, 1 Table

Table of Contents

Table S1. Influent water quality

Week	Water Source	average Total Phosphorous	average Total Nitrogen	average Total Organic Carbon	pH	average Ammonia N	average Nitrate N
		ug/L	ug/L	mg/L		ug/L	ug/L
1	Low nutrient	57.5	185	0		27.1	15
1	High nutrient	214.2	2918	2.9		55.2	2070
2	Low nutrient	49.3	180	1.6		32.7	0
2	High nutrient	339.7	3521	3.4		33.8	2690
3	Low nutrient	47.1	176	0	7.08	30	17
3	High nutrient	149.5	2989	2.6	7.83	43.4	2100
4	Low nutrient	56.7	153	0	7.1	20.4	14
4	High nutrient	145.3	3271	2.3	7.9	43	2710
5	Low nutrient	30.1	305	2.6	7.8	18.4	0
5	High nutrient	646.8	5161	4.4	8.1	810	3930
6	Low nutrient	17.1	154	0	7	25.2	14
6	High nutrient	251.8	3005	3.1	7.7	141	1970
7	Low nutrient	31.6	382	2.8	7.62	39	4
7	High nutrient	231.5	3518	3.5	8.21	90	2480
8	Low nutrient	14.1	143	0	7.16	24.3	18
8	High nutrient	167.9	3283	3.3	7.93	103	2480

Numbers represent the averages between two replicate analyses for each sample. pH values are not available from the first two weeks.

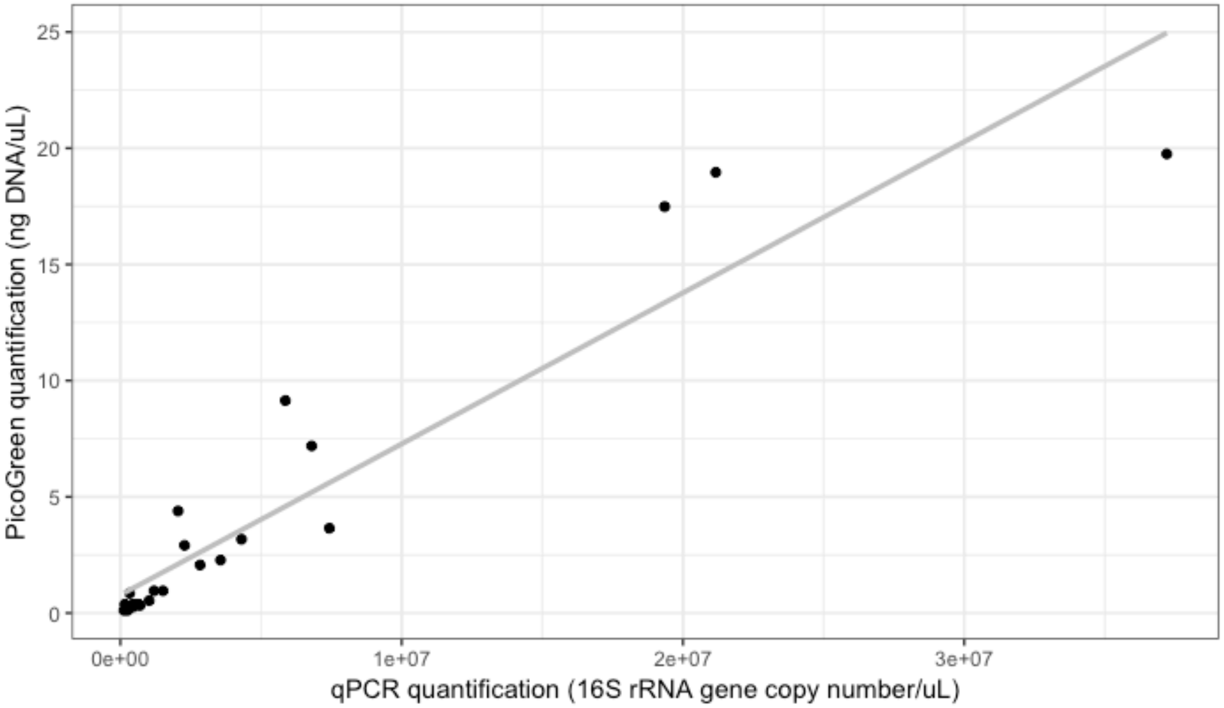

Figure S1. Comparison of DNA quantification by Quant-iT^{TM} PicoGreen^{TM} dsDNA Assay and qPCR targeting the 16S rRNA gene with the primers 515F-806R. The grey line shows the linear regression, intercept = 0.78, slope = 6.5 x 10^{-7}, adjusted $R^2 = 0.88$, and $p < 0.001$.

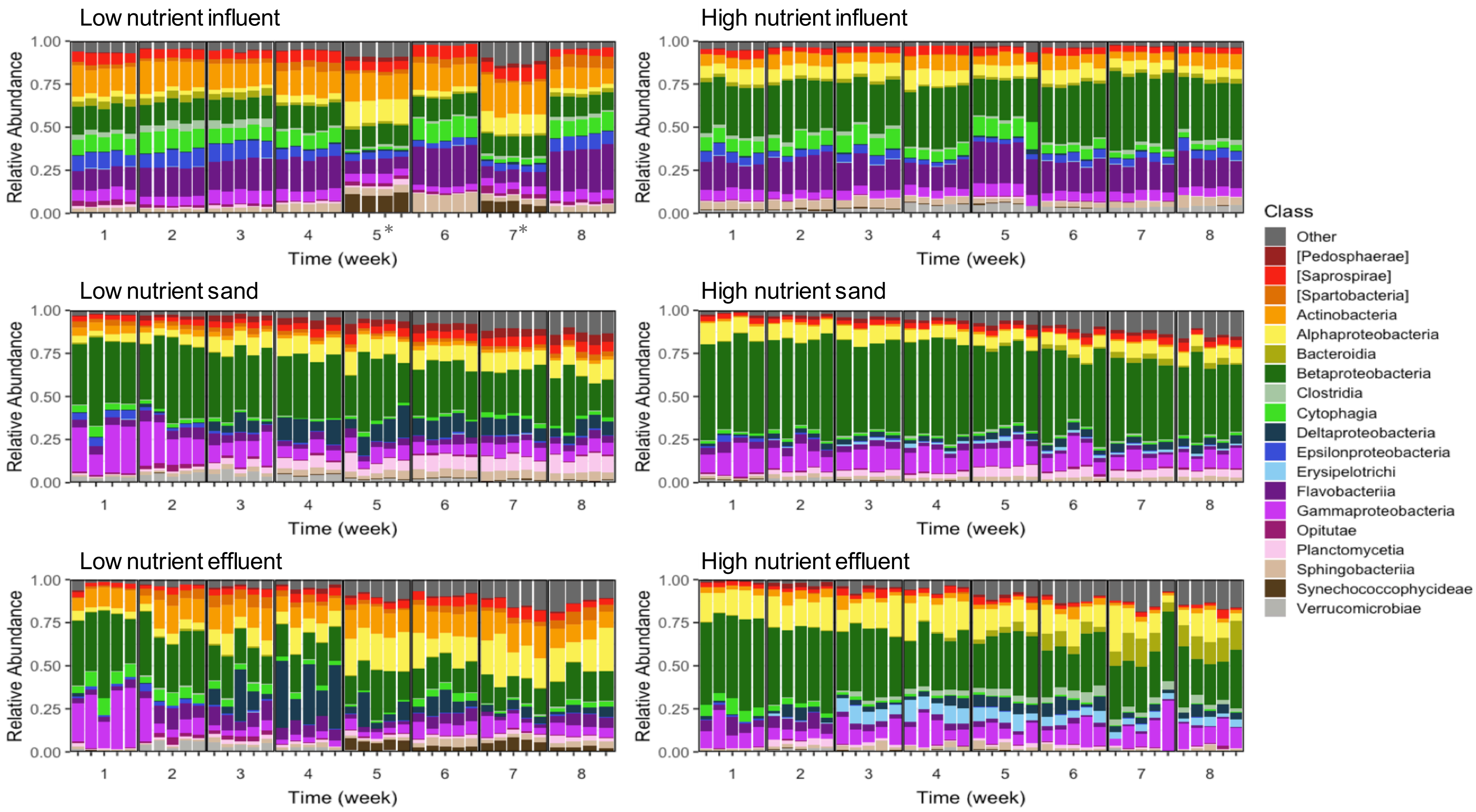

Figure S2. Relative abundance of the 19 most abundant classes over time for the low nutrient (left) and high nutrient (right) water sources for samples from the influent (top), sand (middle), and effluent (bottom) over time. Each bar represents one replicate. * indicate that the low nutrient influent was from a different source during weeks 5 and 7.

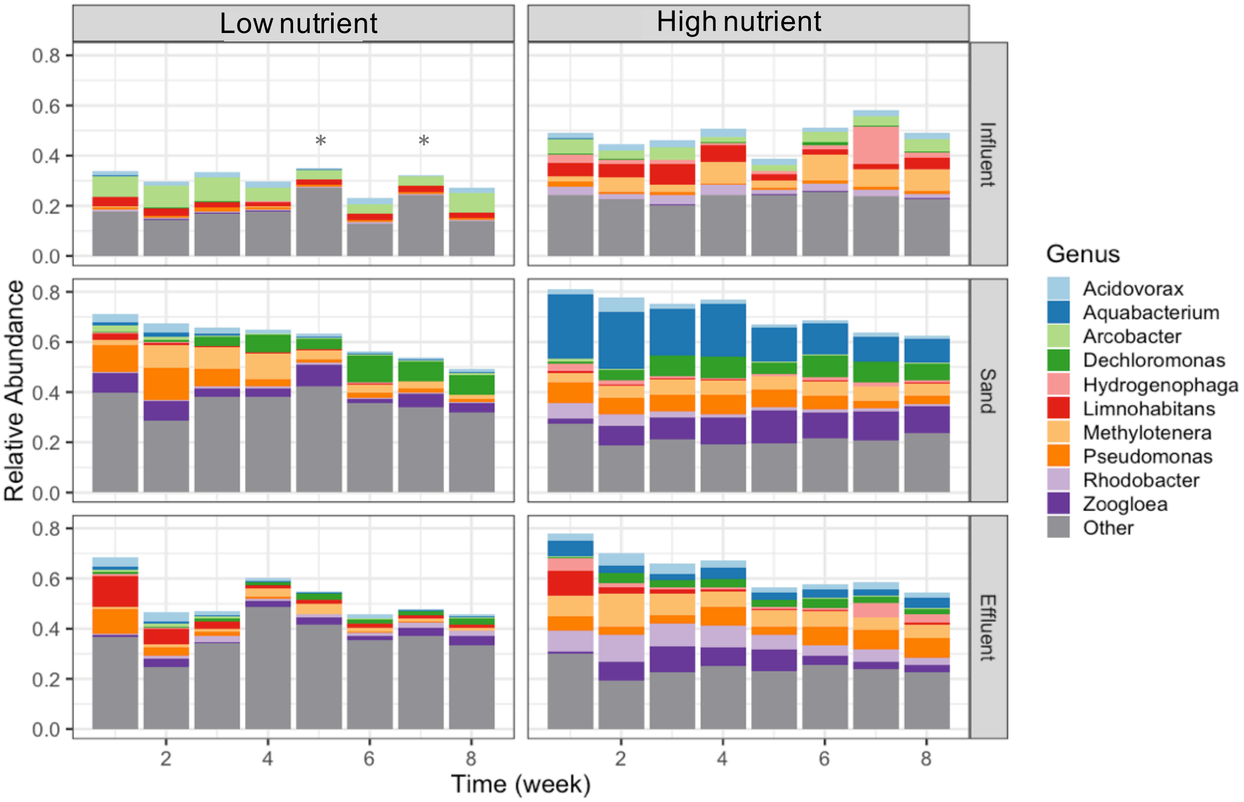

Figure S3. Relative abundance of all Proteobacteria as a fraction of the total microbial community in both source waters for influent, sand, and effluent samples over time. The top 10 most abundant genera are shown by their respective colors with the remaining groups in grey. Each bar represents combined data from four to five replicates. * indicate that the low nutrient influent was from a different water source during weeks 5 and 7.

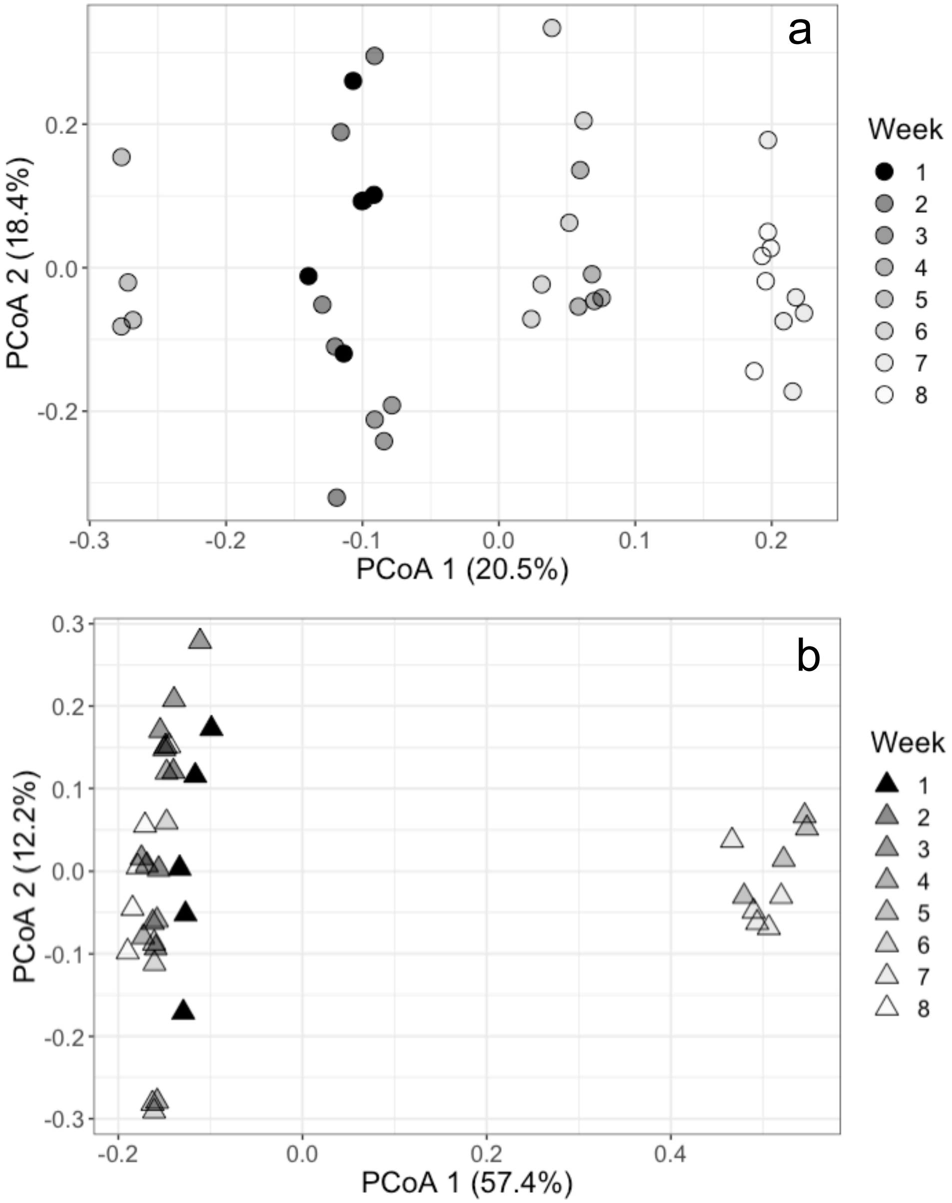

Figure S4. Principal coordinate analyses (PCoA) of microbial communities of influent samples based on pairwise Bray-Curtis dissimilarity over time for high nutrient influent (a) and low nutrient influent (b). Note that the low nutrient influent was from a different source during weeks 5 and 7, which cluster separately.

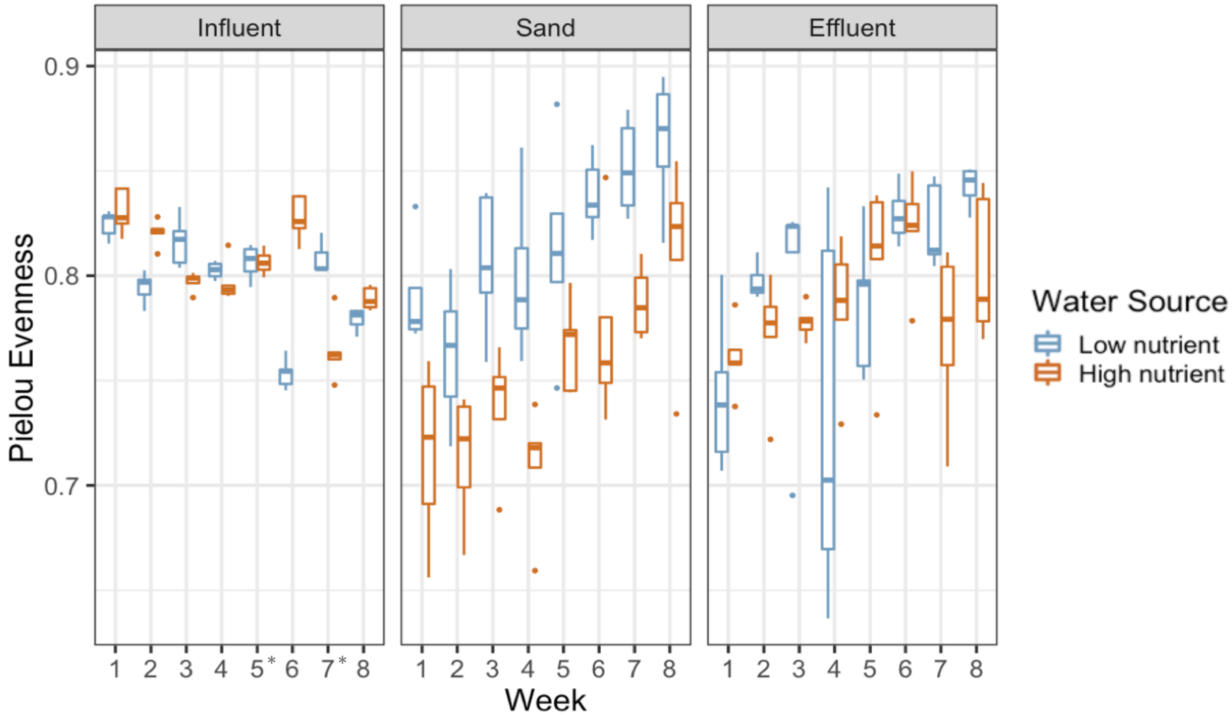

Figure S5. Boxplot of Pielou evenness calculated using a rarefied sequencing depth of 2,122 reads per sample for each water source, sample type, and week. * indicate that the low nutrient influent was from a different source during weeks 5 and 7.

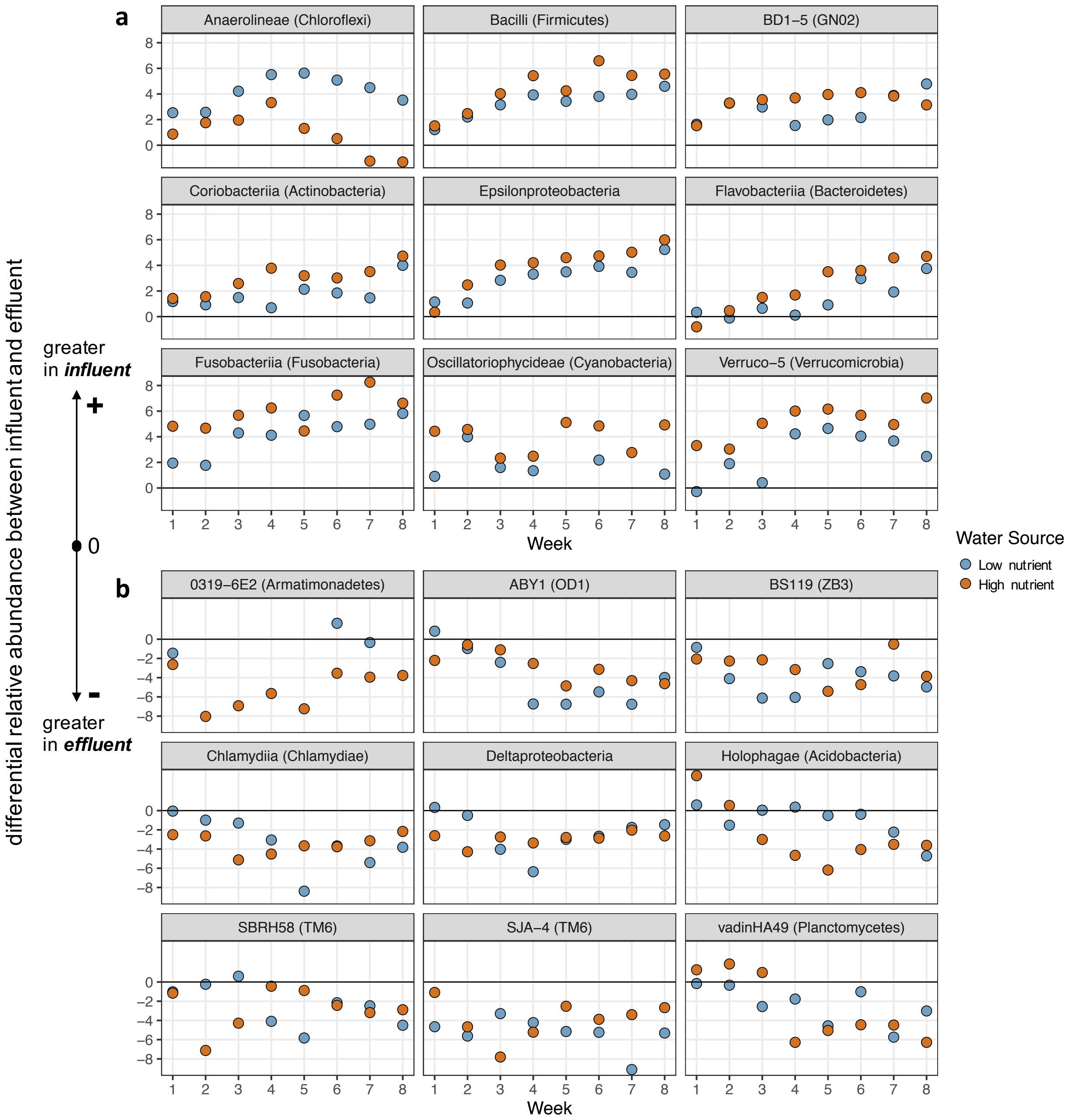

Figure S6. Differential relative abundances between the influent and effluent over time for select bacterial classes from high and low nutrient influents (shown in different colors) and sand filter effluents. Classes that were found to be significantly (FDR <1%) more abundant in the influent (a) or effluent (b) over all time points in both water sources were included.

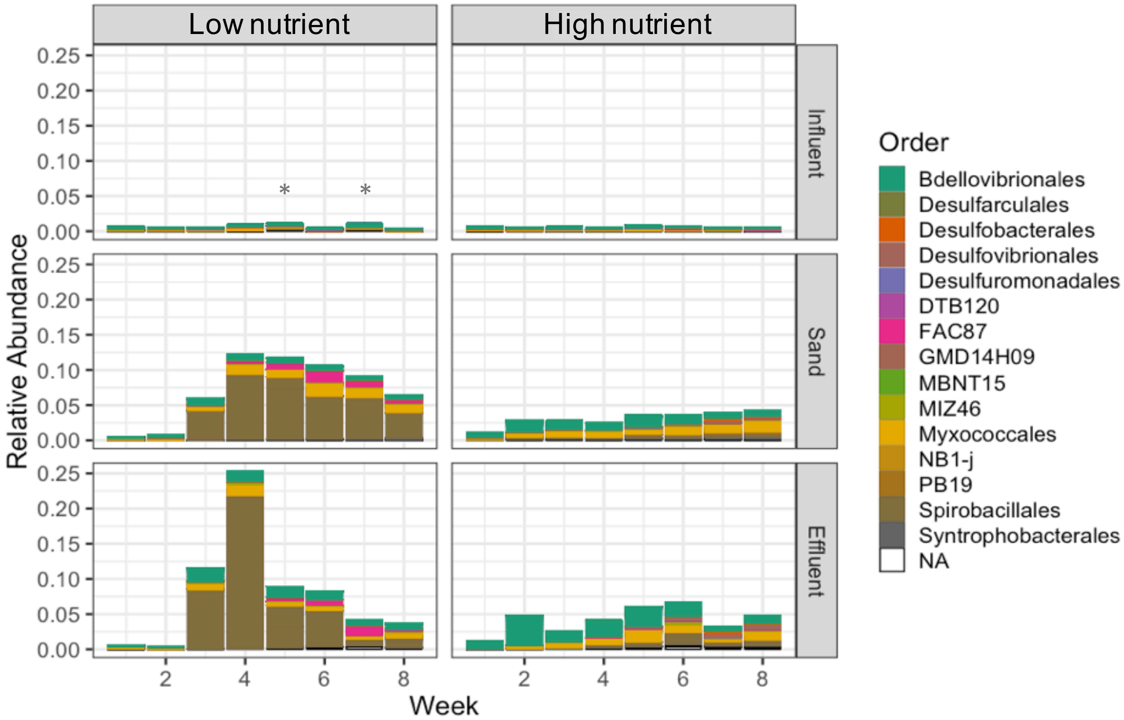

Figure S7. Relative abundance of all Deltaproteobacteria as a fraction of the total microbial community for each water source influent, sand, and effluent samples over time, colored by Order. Each bar represents combined data from four to five replicates. * indicate that the low nutrient influent was from a different water source during weeks 5 and 7.

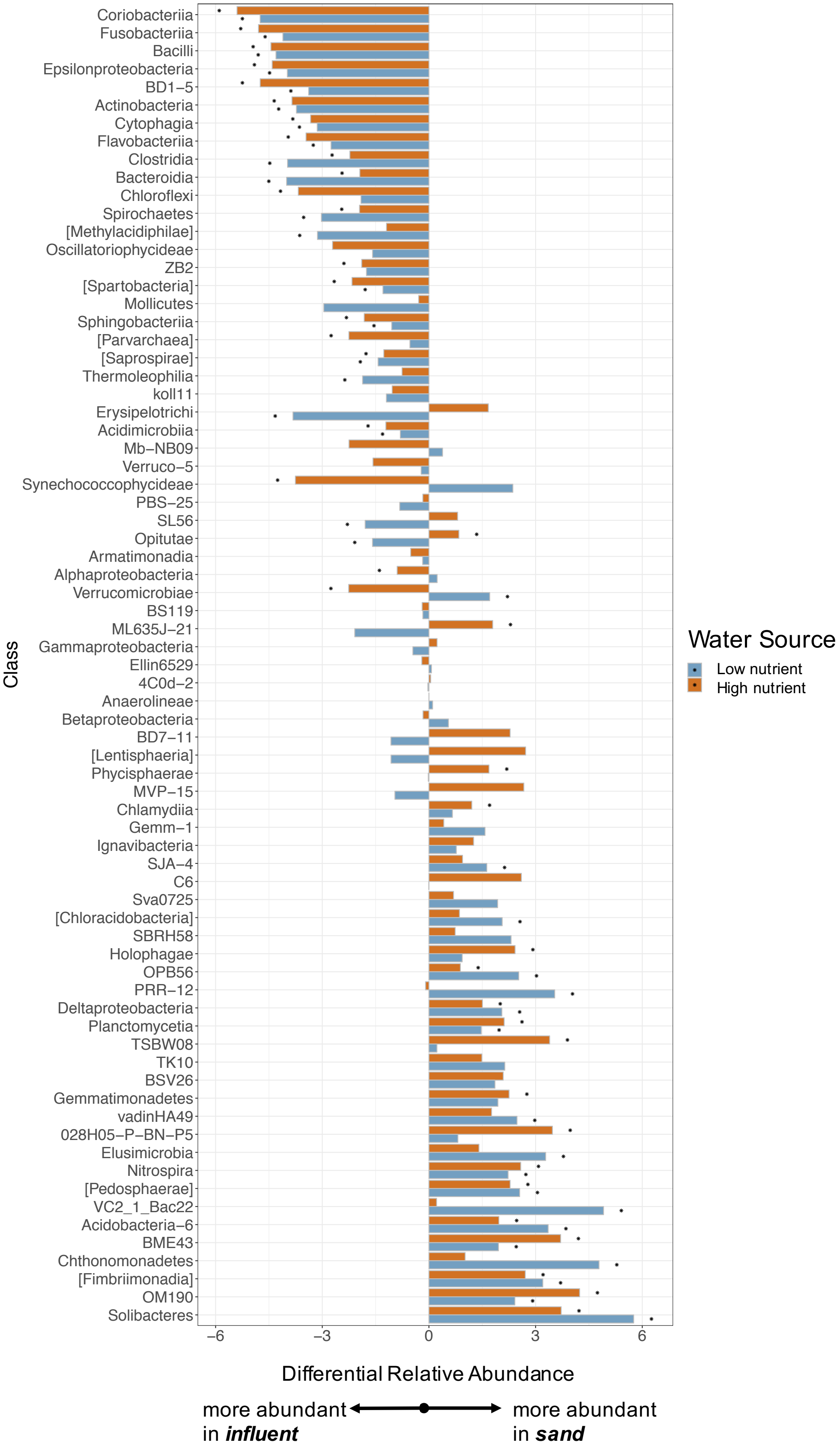
Class
Coriobacteriia
Fusobacteriia
Bacilli
Epsilonproteobacteria
BD1−5
Actinobacteria
Cytophagia
Flavobacteriia
Clostridia
Bacteroidia
Chloroflexi
Spirochaetes
[Methylacidiphilae]
Oscillatoriophycideae
ZB2
[Spartobacteria]
Mollicutes
Sphingobacteriia
[Parvarchaea]
[Saprospirae]
Thermoleophilia
koll11
Erysipelotrichi
Acidimicrobiia
Mb−NB09
Verruco−5
Synechococcophycideae
PBS−25
SL56
Opitutae
Armatimonadia
Alphaproteobacteria
Verrucomicrobiae
BS119
ML635J−21
Gammaproteobacteria
Ellin6529
4C0d−2
Anaerolineae
Betaproteobacteria
BD7−11
[Lentisphaeria]
Phycisphaerae
MVP−15
Chlamydiia
Gemm−1
Ignavibacteria
SJA−4
C6
Sva0725
[Chloracidobacteria]
SBRH58
Holophagae
OPB56
PRR−12
Deltaproteobacteria
Planctomycetia
TSBW08
TK10
BSV26
Gemmatimonadetes
vadinHA49
028H05−P−BN−P5
Elusimicrobia
Nitrospira
[Pedosphaerae]
VC2_1_Bac22
Acidobacteria−6
BME43
Chthonomonadetes
[Fimbriimonadia]
OM190
Solibacteres
−6
−3
0
3
6
Differential Relative Abundance
more abundant in ***influent***
more abundant in ***sand***
Water Source
Low nutrient
High nutrient

Figure S8. Differential relative abundances between the sand and influent of the most abundant microbial classes (>0.01% relative abundance) for each water source across all time points, ordered by the average differential relative abundance for both water sources. Stars indicate statistically significant differences (FDR <1%).